



1 **Application of the LM-BP neural network approach for**
2 **landslide risk assessments**

3 Junnan Xiong^{1,3,*}, Ming Sun², Hao Zhang¹, Weiming Cheng³, Yinghui Yang¹,
4 Mingyuan Sun¹, Yifan Cao¹ and Jiyan Wang¹

5 ¹School of Civil Engineering and Architecture, Southwest Petroleum University, Chengdu, 610500,
6 P.R. China

7 ²Geodetic Third Team, National Administration of Surveying, Mapping and Geo-information of China,
8 Chengdu, 610100, P.R. China

9 ³State Key Laboratory of Resources and Environmental Information System, Institute of Geographic
10 Science and Natural Resources Research, Chinese Academy of Sciences, Beijing 100101, P.R. China

11 *Correspondence to:* Junnan Xiong (neu_xjn@163.com)

12 Running Title: Landslide risk zonation in pipeline areas

13



14 **Abstract.** Landslide disaster is one of the main risks involved with the operation of long-distance oil and
15 gas pipelines. Because previously established disaster risk models are too subjective, this paper presents
16 a quantitative model for regional risk assessment through an analysis of the laws of historical landslide
17 disasters along oil and gas pipelines. Using the Guangyuan section of the Lanzhou-Chengdu-Chongqing
18 (LCC) Long-Distance Products Oil Pipeline (82km) in China as a case study, we successively carried out
19 two independent assessments: a hazard assessment and a vulnerability assessment. We used an entropy
20 weight method to establish a system for the vulnerability assessment, whereas a Levenberg Marquardt-
21 Back Propagation (LM-BP) neural network model was used to conduct the hazard assessment. The risk
22 assessment was carried out on the basis of two assessments. The first, the system of the vulnerability
23 assessment, considered the pipeline position and the angle between the pipe and the landslide (pipeline
24 laying environmental factors). We also used an interpolation theory to generate the standard sample
25 matrix of the LM-BP neural network. Accordingly, a landslide hazard risk zoning map was obtained
26 based on hazard and vulnerability assessment. The results showed that about 70% of the slopes were in
27 high-hazard areas with a comparatively high landslide possibility and that the southern section of the oil
28 pipeline in the study area was in danger. These results can be used as a guide for preventing and reducing
29 regional hazards, establishing safe routes for both existing and new pipelines and safely operating
30 pipelines in the Guangyuan section and other segments of the LCC oil pipeline.

31 **Keywords:** pipeline, landslide, risk, vulnerability, hazard, neural network

32

33 **1. Introduction**

34 By the year 2020, the total mileage of long-distance oil and gas pipelines is expected to exceed 160,000
35 km in China. This represents a major upsurge in the mileage of multinational long-distance oil and gas
36 pipelines (Huo, Wang, Cao, Wang, & Bureau, 2016). The rapid development of pipelines is associated
37 with significant geological hazards, especially landslides, which increasingly threaten the safe operation
38 of pipelines (Wang et al., 2012; Yun & Kang, 2014; Zheng, Zhang, Liu, & Wu, 2012). Landslide disasters
39 cause great harm to infrastructure and human life. Moreover, the wide impact area of landslides restricts
40 the economic development of landslide-prone areas (Ding, Heiser, Hübl, & Fuchs, 2016; Hong, Pradhan,
41 Xu, & Bui, 2015). A devastating landslide can lead to casualties, property losses, environmental damage
42 and long-term service disruptions caused by massive oil and gas leakages (G. Li, Zhang, Li, Ke, & Wu,
43 2016; Zheng et al., 2012). Generally, pipeline failure or destruction caused by landslides is much more
44 deleterious than the landslides themselves, which makes it important to research the risk assessment of
45 geological landslide hazards in pipeline areas (Inaudi & Glisic, 2006; Mansour, Morgenstern, & Martin,
46 2011).

47 Natural disaster risk comprises a combination of natural and social attributes (Atta-Ur-Rahman &
48 Shaw, 2015). The United Nations Department of Humanitarian Affairs expresses natural disaster risk as
49 a product of hazards and vulnerabilities (Rafiq & Blaschke, 2012; Sari, Innaqa, & Safrilah, 2017). In
50 recent years, progress in geographic information systems (GIS) and remote sensing (RS) technologies
51 have greatly enhanced our ability to evaluate the potential risks that landslides pose to pipelines (Akgun,



52 Kincal, & Pradhan, 2012; B. Li & Gao, 2015; Sari et al., 2017). The disaster risk assessment model has
53 been widely recognized and applied by experts and scholars all over the world. Landslide risk assessment
54 can take the form of a qualitative (Wu, Tang, & Einstein, 1996), quantitative (Ho, Leroi, & Roberds,
55 2000) or semi-quantitative assessment (Yingchun Liu, Shi, Lu, Xiao, & Wu, 2015) according to actual
56 demand. Quantitative methods and models that have been proposed for the assessment can be divided
57 into methods of statistical analysis (Sari et al., 2017), mathematical models (Akgun et al., 2012) and
58 machine learning (He & Fu, 2009). However, most of these methods are subjective, which could affect
59 the accuracy and reasonableness of the evaluation (Fall, Azzam, & Noubactep, 2006; Sarkar & Gupta,
60 2005). This shortcoming can be overcome through the artificial neural network, especially the mature
61 Back Propagation (BP) Neural Network that is widely used in function approximation and pattern
62 recognition (Ke & Li, 2014; P. L. Li, Tian, & Li, 2013; Su & Deng, 2003). The evaluation index system
63 generally includes disaster characteristics, disaster prevention and pipeline attributes (J. Li, 2010;
64 Shuiping Li, 2008). The fault tree analysis, fuzzy comprehensive evaluation and the grey theory are used
65 to evaluate the failure probability of the system through index weight and scoring (Shi, 2011; Ye, Jiang,
66 Yao, Xia, & Zhao, 2013). In previous studies, pipeline vulnerability evaluation indexes only considered
67 the pipeline itself, and the relationship between the pipeline and environment was rarely examined (Feng,
68 Zhang, & Zhang, 2014; Shuiping Li, 2008; Yingchun Liu et al., 2015). In this paper, the interaction
69 between landslide hazards and the pipeline itself was considered, which improved the quantitative degree
70 of the evaluation.

71 Based on the theory of the LM-BP neural network, a standard sample matrix was developed using the
72 interpolation theory after an analysis of the distribution characteristics of landslides that occurred in the
73 study area was performed and a regional landslide hazards assessment was completed. Considering the
74 interaction between landslide disasters and the pipeline itself, the pipeline vulnerability evaluation in the
75 landslide area was realized using the entropy weight method. This paper established a risk assessment
76 model and methods for assessing landslide geological hazards of oil pipelines by comprehensively
77 utilizing GIS and RS technology, which together improved the quantitative degree of the assessment.

78 2. Study Area

79 The study area was Guangyuan City in the Sichuan province, which was further restricted to the area
80 from 105°15' to 106°04' E and 32°03' to 32°45' N, straddling 19 townships in five counties from south to
81 north (Figure 1). The Lanzhou-Chengdu-Chongqing (LCC) Products Oil Pipeline is China's first long-
82 distance pipeline. It begins in Lanzhou City and runs through the Shanxi and Sichuan provinces (Hao &
83 Liu, 2008). Our study area covered sloped areas of the range with 5 km on both sides of the Guangyuan
84 section (82 km) of the oil pipeline. The pipeline within the K558-K642 mileages may be affected by the
85 slope areas. The Guangyuan section, located in northern Sichuan, is a transitional zone from the basin to
86 the mountain. It features a terrain of moderate and low mountains, crisscrossed networks of ravines and
87 a strong fluvial incision. Altitudes in this area range from 328 m to 1505 m. The study area has a
88 subtropical monsoon climate with four distinctive seasons and annual precipitation measuring about 900
89 mm to 1,000 mm. Moreover, two large unstable faults (the Central Fault of Longmen Mountain and
90 Longmen Mountain's Piedmont Fault Zone) make the area geologically unstable and prone to frequent



91 geological hazards (Shiyuan Li et al., 2012). Guangyuan, through which the pipeline passes, has a high
92 incidence of landslides, some of which have happened 300 times in the Lizhou and Chaotian districts
93 (Zhang, Shi, Gan, & Liu, 2011). In this area, landslide geological hazards seriously threaten the safe
94 operation of the LCC oil pipeline.

95 **3. Data Sources**

96 Landslide hazard assessment, pipeline vulnerability assessment and geological hazard risk assessment of
97 the landslide pipeline were made successively. Digital elevation model (DEM) data with 30 m accuracy
98 was sourced from the Geospatial Data Cloud (<http://www.gscloud.cn/>). Precipitation data was
99 downloaded from the dataset of annual surface observation values in China between the years 1981 to
100 2010, as published by the China Meteorological Administration (<http://data.cma.cn/>). This data was
101 collected from 18 meteorological observatories near and within the study area and interpolated using the
102 kriging method (at a resolution of 30 m × 30 m). Geological maps and landslide data (historical landslides)
103 in the study area were obtained from the Sichuan province's geological environmental monitoring station.
104 RS images (GF-1, multispectral 8 m, resolution 2 m) were provided by the Sichuan Remote Sensing
105 Center.

106 The location of the middle line of the pipeline was detected through the direct connection method (i.e.,
107 the transmitter's output line was directly connected to the metal pipeline) using an RD8000 underground
108 pipeline detector. Pipeline midline coordinates were measured using total network Real Time Kinematic
109 technology, and simultaneously, the coordinates of the pipe ancillary facilities (including test piles,
110 mileage piles and milestones) were acquired. Mileage data obtained through inner pipeline detection was
111 derived from the China Petroleum Pipeline Company.

112 **4. Methods**

113 **4.1 Assessment unit**

114 Division precision and the scale of the slope unit (i.e., the basic element for a regional landslide hazard
115 assessment) were in keeping with the results of the evaluation (Qiu, Niu, ZhaoYannan, & Wu, 2015). A
116 total of 315 slope units were divided using hydrologic analysis in ArcGIS (v. 10.4) (Fig. 2a). The
117 irrational unit was artificially identified and modified by comparing GF-1 satellite remote sensing
118 images. Boundary correction, fragment combination and fissure filling were used for modification.
119 The object of the pipeline vulnerability assessment in the landslide area was the pipeline. Considering
120 both previous research and the particulars of the research object, we used a comprehensive
121 segmentation method based on GIS to divide the pipelines in our study. A total of 180 pipes were
122 divided in the study area, of which the longest was about 1.7 km, and the shortest was only about 10 m
123 (Fig. 2b).

124 **4.2 Assessment factors**

125 Based on selection principles of the indicator system and the formation mechanism of landslide
126 geological hazards, as few indicators as possible were selected to reflect the degree of danger posed by
127 the landslide as accurately as possible (Avalon Cullen, Al-Suhili, & Khanbilvardi, 2016; Jaiswal, Westen,



128 & Jetten, 2010; Ray, Dimri, Lakhera, & Sati, 2007). The internal factors in these indicators of the paper
129 included topography, geological structure, stratigraphic lithology and surface coverage. Similarly, the
130 external factors included mean annual precipitation (MAP) and the coefficient of the variation of annual
131 rainfall (CVAR). The correlations between indicators were analyzed using R (v. 3.3.1), and the results
132 showed a significant correlation between MAP and CVAR ($R = 0.99$) and between NDWI and NDVI (R
133 $= 0.87$). Based on correlation and standard deviation, CVAR and NDWI were eliminated from the
134 original evaluation system for landslide hazard assessment in the pipeline area (Table 1).

135 Generally, the evaluation index of pipeline vulnerability as it relates to the relationship between a pipeline
136 and its surrounding environment is rarely considered. The evaluation indicators in this paper were refined
137 to include pipeline parameters and the spatial relationship between a pipeline and landslide. The pipelines
138 in the study area were based in mountainous areas and had been running for many years. All of these
139 pipelines consisted of high-pressure pipes that were made of steel tubes and had a diameter of 610 mm
140 for conveying oil. In keeping with the theory of the entropy weight method, these indicators (e.g.,
141 pressure, materials, diameter and media) were not included in the final evaluation system used to
142 determine pipeline vulnerability.

143 4.3 LM-BP neural network Model

144 The LM algorithm, also known as the damped least square method, has the advantage of local fast
145 convergence. Its strong global searching ability contributes to the strong extrapolation ability of the
146 trained network. The BP neural network model, optimized by the LM algorithm, was used to evaluate
147 the regional landslide hazard in this study. MATLAB 2014 with the *trainlm* training function was used
148 to implement the LM-BP neural network.

149 Data from 106 landslide disasters was collected near the research area. Of these landslides, 23 were
150 within the region of the study area. Most of the landslides located outside the study area were less than
151 20 km away from the pipeline. Due to comparable environmental conditions, these landslides could still
152 help us identify the relationship between landslides and environment factors. In light of the frequency
153 distribution of each evaluation indicator (Fig. 3), the landslide hazard grade corresponding to each
154 interval of the indicators was divided, and then the hazard degree monotonicity in each interval was
155 decided. For this study, the landslide hazard grade was divided into four levels: low (I), medium (II),
156 high (III) and extremely high (IV).

157 On the basis of the classification criteria of the evaluation indicators used to predict landslide hazard
158 degree and the functional relationship between the evaluation indicators and landslide probabilities,
159 standard samples (training samples and test samples) were built using a certain mathematical method.
160 The training samples and test samples were evaluated using similar construction methods but with
161 different sample sizes. Finally, the indicator data was normalized, it was entered into the LM-BP neural
162 network for simulation and 315 slope unit landslide hazard values were output.

163 4.4 Vulnerability assessment model for pipelines

164 The vulnerability evaluation model of pipelines in the landslide area was established using the entropy
165 weight method, which overcame the shortcomings of the traditional weight method that does not consider
166 the different evaluation indexes and the excessive human influence on the process of evaluation (Gao,



167 Li, Wang, Li, & Lin, 2017; Pal, 2014). Pipeline defect density was obtained from the pipeline internal
168 inspection data, which consisted of both mileage data that needed to be converted into three-dimensional
169 coordinate data and pipeline center line coordinate data obtained through C# programming. In addition,
170 the main slide direction of the landslide was replaced by the slope direction that was extracted by DEM.
171 The coordinate azimuth of the pipe section was extracted using the linear vector data of each pipe section,
172 and the angle between the pipeline and the slope was calculated using the mathematical method. The
173 calculation process was solved in the VB language on ArcGIS using second development functions.
174 Finally, the entropy weight of 5 indexes was calculated by programming in MATLAB 2014. The entropy
175 weight calculation results for pipeline landslide vulnerability assessment are shown in Table 2. Pipeline
176 vulnerability in landslide area was calculated using the following formula:

$$177 \quad H_j = \sum_{i=1}^m w_i r_{ij} \quad (1)$$

178 where H_j is the evaluation value of the pipeline section's vulnerability; w_i is the weight of the evaluation
179 index; and r_{ij} represents the i^{th} evaluation index values of j^{th} pipe sections.

180

181 **5 Results and comparison**

182 **5.1 Regional landslide hazard assessment**

183 The LM-BP neural network was trained and the network was stopped after 182 iterations. An RMSE
184 value of 9.93e-09 indicated that the goal of precision had been reached. Through the simulation of the
185 network test, none of the absolute error values of test data (20 groups) were found to be greater than 0.02;
186 this result aligned with our expectation of the precision of the landslide hazard assessment. The landslide
187 hazard grade was divided into four levels by using the equal interval method at intervals of 0.25. The
188 safe section (low hazard) was located in the central part of the study area. The dangerous (high hazard)
189 section was located north and south (Fig. 4). In the study area, most of the exposed rock was dominated
190 by shale, which belonged to the easy-slip rock group.

191 Average altitude ranged from 450 m to 1400 m, and the relative height difference was greater than 80
192 m, with the slope between 15 ° and 35 °. Based on an overlay analysis of historic landslides within the
193 study area, and hazard zonation maps, we surmised that the probability of landslides in the study area
194 was extremely high, and that 87% of the landslides occurred in the medium-, high-, and extremely high-
195 hazard areas. Among these landslides, three were located in low-hazard areas, which accounted for 13%
196 of the landslide disaster sites, five occurred in medium-hazard areas (accounting for 21.7% of disaster
197 sites), seven occurred in high-hazard areas (accounting for 30.4% of sites) and eight occurred in
198 extremely high-hazard areas (accounting for 34.8% of sites). The evaluation results were found to
199 accurately reflect the trends and rules of distribution of landslides in the study area. The number and area
200 of slopes in high-hazard and extremely high-hazard areas accounted for about 70% of the total (Table 3).
201 The probability of landslide occurrence in the study area was generally high, which was consistent with
202 the fact that the region was landslide-prone.

203 **5.2 Vulnerability assessment for oil pipeline in landslide area**



204 The equal interval of 0.25 was used to divide the pipeline vulnerability level into four grades to obtain
205 the pipeline vulnerability zonation of the study area (Fig. 5). The pipeline in the northern part of the study
206 area was given a low vulnerability grade, while the situation in the south of the region is more serious.
207 The number, length and percentage of pipeline segments with different grade vulnerabilities are shown
208 in Table 4. The number and length of pipeline segments in highly vulnerable areas (III) and extremely
209 vulnerable areas (IV) accounted for about 12% of the total.

210 5.3 Risk assessment for oil pipeline in landslide area

211 According to natural disaster risk expressions released by the UN, the definition of risk may be expressed
212 as the product of landslide hazard in a pipeline area and pipeline vulnerabilities in the landslide area. The
213 risk degrees were distinguished using the equal interval method, and four grades were generated. Where
214 the comprehensive risk assessment value was within 0 to 0.0625, the corresponding risk grade was Grade
215 I; the corresponding risk grades with the values of 0.0625 to 0.25, 0.25 to 0.5625 and 0.5625 to 1.0 were
216 Grade II, III and IV, respectively. The risk grade of each section of the pipeline within the research area
217 is shown in Fig. 6.

218 The number of sections with a high-risk grade was 33, which accounted for 18.33% of all pipeline
219 sections and represented 16.57% of the total pipeline length of 13.461 km). There were 4 sections with
220 extremely high-risk grade, which accounted for 2.22% of all sections and represented 3.31% of the total
221 pipeline length of 2.538 km. The section number and length of pipelines lying in high-risk (III) and
222 extremely high-risk (IV) areas accounted for 20% of the total pipeline length, and the risk grade of
223 pipelines inside Qingchuan and Jian'ge County was relatively high.

224 5.4 Analysis of risk assessment results

225 Large or huge landslides were common in areas that we categorized as extremely high risk, which we
226 defined as those that were geologically evolving or had experienced obvious deformations within the last
227 2 years with still visible cracks. These pipelines were subject to dangers at any time, as the pipelines
228 within the areas prone to landslides were found to contain many defects or extensive damage. These
229 areas also posed considerable threats; for example, pipeline ruptures or breaks could lead to leakages or
230 serious deformations that cause transportation failure. Because these are unacceptable events, risk
231 prevention and control measures must be taken in a short time. Pipelines with extremely high risk were
232 mainly distributed in the following areas: (1) Xiasi Village in Xiasi County (Pile No. K628-K630); (2)
233 Shiweng Village-Maliu Village of Xiasi County (Pile No. K635-K637). This section lay in the south of
234 the research area, with an altitude of 500 m to 750 m. Here, the slope conditions affected the distribution
235 of groundwater pore pressure and the physical and mechanical characteristics of the rock and soil in three
236 areas: vegetation cover, evaporation and slope erosion. Ultimately, these three factors affected slope
237 stability (Luo & Tan, 2011). Vertical and horizontal ravines have also been seen in this section, with
238 a relative height difference greater than 100 m and slope between 15° to 35°. Slope degrees with
239 obvious changes had a great influence on slope stability (Chang & Kim, 2004; Hu, Xu, Wang, Asch, &
240 Hicher, 2015). The exposed rocks in this area were mainly shale and belonged to the sliding-prone
241 rock group. Rock type and interlayer structure were found to be important internal indicators that a
242 landslide could occur (Guzzetti, Cardinali, & Reichenbach, 1996; Xiang et al., 2010; Xin, Chong, &



243 Dai, 2009). The distance between the fault and the pipeline in the section was about 2 km with a
244 NDVI of about 0.75 and MAP of about 970 mm. Faulted zones and nearby rock and earth masses
245 that were destroyed in a geologic event reduced the integrity of a slope, and the faults and important
246 groundwater channels could also cause deformation and damage of a slope (Yinghui Liu, 2009). The
247 pipelines in these areas exhibited many defects. Most pipelines passed through the slope in an inclined
248 or horizontal way, an attribute that typically increased the risk of a landslide occurring.

249 In high-risk areas, small or moderate landslides commonly occurred in areas that we categorized as
250 high risk. They were in deformation, or had obvious deformation recently (within 2 years), such as
251 obvious cracks, subsidence or tympanites on the landslide and even shear. The pipelines in these areas
252 had defects and were buried at a shallow depth. If a landslide occurred in this pipeline area, it could cause
253 pipe suspension, floating and damage. It could also contribute to a small to moderate leakage of the
254 medium. However, damaged pipes can be welded or repaired. Monitoring is critical in high-risk areas.
255 In our study, the pipeline high-risk area was defined by the following areas: (1) Xiasi Town Xiasi Village-
256 Shiweng Village (pipe No. K622-K633). (2) Xiasi Town Maliu Village Jinzishan Xiangdasang Village
257 (pipe No. K635-K642). This area was located in the south of the pipe, which was buried in the study area.
258 The altitude of the study area was between 450 m and 800 m, the relative elevation difference was over
259 100m and the slope was between 15 ° and 40 °. Most of the outcrops in this area were quartz sandstone,
260 which belonged to the easy-sliding rock group. The pipes in this area were about 2.5 km away from faults.
261 The NDVI was about 0.6 to 0.8, and MAP was about 970 nm. Pipes showed many defects, most of them
262 either crossing the slope or lying in the center of slope. All of the above factors provided sufficient
263 conditions for the formation of landslide.

264 In the medium-risk areas, only small landslides were found to occur, and we observed no sign of
265 deformation. But through the analysis of geological structure, topography and landform, we found the
266 area to demonstrate a tendency for developing landslides. The pipes in this risk area exhibited almost no
267 faults and were buried deep beneath the ground. However, under bad conditions, the landslides in these
268 areas could also affect the pipes' safety, causing the pipes to become exposed or deformed. These areas
269 need simple monitoring. For our study, medium-risk areas were defined as follows: (1) Sanlong village
270 of Dongxihe township-Panlong town Dongsheng village (pipe No. K559-K593). (2) Panlong town
271 Qinlao village-Wu'ai village (pipe No. K595-K597). (3) Baolun town Laolin'gou village-Xiasi town
272 Youyu village (pipe No. K599-K630).

273 In the low-risk areas, landslides didn't occur under ordinary conditions, but they could occur if a strong
274 earthquake hit or if the area experienced continuous or heavy rain. The pipes in low-risk areas showed
275 no defects and were buried very deep. They were also located far away from areas affected by landslides.
276 Therefore, landslides in these areas caused no obvious damage to the pipes, and few threatened the safety
277 of pipes. However, regular inspection is necessary to ensure that the pipes continue to operate safely. The
278 pipe low-risk area were defined as follows: (1) Panlong town Dongsheng village-Qinlao village (pipe
279 No. K591-K597). (2) Baolun town Xiaojia village-Baolun town Laolin'gou village (pipe No. K599-
280 K608).

281 Through comprehensive analysis of each risk level area, we compiled a list of pipeline landslide risks
282 (Table 6). This list describes each landslide risk level in four respects: pipeline risk, landslide hazard,



283 pipeline vulnerability and risk control measures.

284 **5 Results and comparison**

285 The faults inherent to traditional landslide risk assessment include excessive human influence, failure of
286 pipeline vulnerability assessments to consider the interaction between landslide disaster and pipeline
287 ontology and the low quantification degree of risk assessment results.

288 Taking the Guangyuan section (82 km) of the LCC oil and gas pipeline as an example, we used GIS
289 and RS technology to establish a regional landslide hazard assessment model based on the LM-BP neural
290 network. We determined that there were 112 and 108 slopes in high-hazard and extremely high-hazard
291 areas that accounted for 33.18% and 40.46% of the total area of the study area, respectively. Then, we
292 established the model of pipeline vulnerability evaluation based on the entropy weight method by
293 combining the pipeline body and the environmental information. The number and length of pipe
294 segments in the highly vulnerable (III) and extremely vulnerable area (IV) accounted for about 12% of
295 the total. Finally, based on the hazard assessment and the vulnerability assessment, we completed the
296 risk assessment and risk division of the oil pipeline, thus forming a geological disaster risk assessment
297 model and a method for oil pipeline and landslide risk assessment. The risk assessment results
298 demonstrated that the number and length of high-hazard and extremely high-hazard pipeline segments
299 represented 20% of the total. Similarly, the pipeline risk within Qingchuan and Jian'ge Counties was
300 relatively high. Our pipeline landslide risk assessment has laid a foundation for the future study of
301 pipeline safety management and pipeline failure consequence loss assessment.

302

303 **Acknowledgments**

304 The study has been funded by the Strategic Priority Research Program of Chinese Academy of Sciences
305 (XDA20030302), IWHR(China Institute of Water Resources and Hydropower Research) National
306 Mountain Flood Disaster Investigation Project (SHZH-IWHR-57), Southwest Petroleum University Of
307 Science And Technology Innovation Team Projects (2017CXTD09) and the Study on temporal and
308 spatial differentiation of historical mountain flood disasters in Fujian province (NDMBD2018003).

309

310



311 **References**

- 312 Akgun, A., Kincal, C., and Pradhan, B.: Application of remote sensing data and GIS for landslide risk
313 assessment as an environmental threat to Izmir city (west Turkey). *Environmental Monitoring &*
314 *Assessment*, 184(9), 5453-5470. [https://doi: 10.1007/s10661-011-2352-8](https://doi.org/10.1007/s10661-011-2352-8) 2012.
- 315 Atta-Ur-Rahman, and Shaw, R. (2015). *Hazard, Vulnerability and Risk: The Pakistan Context*: Springer
316 Japan.
- 317 Avalon Cullen, C., Al-Suhili, R., and Khanbilvardi, R.: Guidance Index for Shallow Landslide Hazard
318 Analysis. *Remote Sensing*, 8(10), 866. [https://doi: 10.3390/rs8100866](https://doi.org/10.3390/rs8100866), 2016.
- 319 Chang, H., and Kim, N. K.: The evaluation and the sensitivity analysis of GIS-based landslide
320 susceptibility models. *Geosciences Journal*, 8(4), 415-423. [https://doi: 10.1007/BF02910477](https://doi.org/10.1007/BF02910477), 2004.
- 321 Ding, M., Heiser, M., Hübl, J., and Fuchs, S.: Regional vulnerability assessment for debris flows in
322 China—a CWS approach. *Landslides*, 13(3), 537-550. [https://doi: 10.1007/s10346-015-0578-1](https://doi.org/10.1007/s10346-015-0578-1) 2016.
- 323 Fall, M., Azzam, R., and Noubactep, C.: A multi-method approach to study the stability of natural slopes
324 and landslide susceptibility mapping. *Engineering Geology*, 82(4), 241-263. 2006.
- 325 Feng, W., Zhang, T., and Zhang, Y.: Evaluating the stability of landslides in xianshizhai village and the
326 pipeline vulnerability with their action. *Journal of Geological Hazards & Environment Preservation*.
327 2014.
- 328 Gao, C. L., Li, S. C., Wang, J., Li, L. P., and Lin, P.: The Risk Assessment of Tunnels Based on Grey
329 Correlation and Entropy Weight Method. *Geotechnical & Geological Engineering*(4), 1-11. [https://doi: 10.1007/s10706-017-0415-5](https://doi.org/10.1007/s10706-017-0415-5) 2017.
- 331 Guzzetti, F., Cardinali, M., and Reichenbach, P.: The Influence of Structural Setting and Lithology on
332 Landslide Type and Pattern. *Environmental & Engineering Geoscience*, 2(4), 531-555. 1996.
- 333 Hao, J., and Liu, J.: Zonation of Danger Degree of Geological Hazards over Lanzhou-Chengdu-
334 Chongqing Products Pipeline. *Oil & Gas Storage & Transportation*. 2008.
- 335 He, Y., and Fu, W.: Application of fuzzy support vector machine to landslide risk assessment. *Journal of*
336 *Natural Disasters*, 18(5), 107-112. 2009.
- 337 Ho, K., Leroi, E., and Roberds, B.: *Quantitative Risk Assessment : Application, Myths and Future*
338 *Direction*. 2000.
- 339 Hong, H., Pradhan, B., Xu, C., and Bui, D. T.: Spatial prediction of landslide hazard at the Yihuang area
340 (China) using two-class kernel logistic regression, alternating decision tree and support vector machines.
341 *Catena*, 133, 266-281. [https://doi: 10.1016/j.catena.2015.05.019](https://doi.org/10.1016/j.catena.2015.05.019) 2015.
- 342 Hu, W., Xu, Q., Wang, G. H., Asch, T. W. J. V., and Hicher, P. Y.: Sensitivity of the initiation of debris
343 flow to initial soil moisture. *Landslides*, 12(6), 1139-1145. [https://doi: 10.1007/s10346-014-0529-2](https://doi.org/10.1007/s10346-014-0529-2) 2015.
- 344 Huo, F., Wang, W., Cao, Y., Wang, F., and Bureau, C. P.: China's Construction Technology of Oil and Gas
345 Storage and Transportation and Its Future Development Direction. *Oil Forum*. 2016.
- 346 Inaudi, D., and Glisic, B.: Reliability and field testing of distributed strain and temperature sensors.
347 *Proceedings of SPIE - The International Society for Optical Engineering*, 6167(14), 2586-2597.
348 [https://doi: 10.1117/12.661088](https://doi.org/10.1117/12.661088) 2006.
- 349 Jaiswal, P., Westen, C. J. V., and Jetten, V.: Quantitative landslide hazard assessment along a
350 transportation corridor in southern India. *Engineering Geology*, 116(3), 236-250. [https://doi: 10.1016/j.enggeo.2010.09.005](https://doi.org/10.1016/j.enggeo.2010.09.005), 2010.
- 352 Ke, F., and Li, Y.: *The forecasting method of landslides based on improved BP neural network*.
353 *Geotechnical Investigation & Surveying*. 2014.
- 354 Li, B., and Gao, Y. (2015). Application of the improved fuzzy analytic hierarchy process for landslide



- 355 hazard assessment based on RS and GIS. Paper presented at the International Conference on Intelligent
356 Earth Observing and Applications.
- 357 Li, G., Zhang, P., Li, Z., Ke, Z., and Wu, G.: Safety length simulation of natural gas pipeline subjected
358 to transverse landslide. 2016.
- 359 Li, J. (2010). Wenchuan Earthquake and Secondary Geological Hazard Assessment Based on RS/GIS
360 Technology. (Master), China University of Geosciences, Beijing, China.
- 361 Li, P. L., Tian, W. P., and Li, J. C.: Analysis of landslide stability based on BP neural network. Journal of
362 Guangxi University. 2013.
- 363 Li, S. (2008). The Risk Assessment Study on the Environmental Geological Hazards along the West-East
364 Nature Gas Pipeline. (Mater), SouthWest JiaoTong University, Chengdu, China.
- 365 Li, S., Jian, j., Wu, Z., Li, S., Li, H., Bai, K., Ke, Q., Xu, Y., and Hu, Y.: A Design of the Geo-
366 Environmental Management Database System for Guangyuan City Journal of Geological Hazards and
367 Environment Preservation, 23(3), 7. 2012.
- 368 Liu, Y. (2009). The characteristic and evaluation of collapse and landslide disaster along du-wen highway
369 in Wenchuan earthquake region. (Master), Lanzhou University, Lanzhou.
- 370 Liu, Y., Shi, Y., Lu, Q., Xiao, H., and Wu, S.: Risk Assessment of Geological Disasters in Single Pipe
371 Based on Scoring Index Method: A Case Study of Soil Landslide. Natural Gas Technology & Economy.
372 2015.
- 373 Luo, Z. F., and Tan, D. J.: Landslide Hazard Evaluation in Debris Flow Catchment Area Based on GIS
374 and Information Method. China Safety Science Journal, 21(11), 144-150. [https://doi:
375 10.1631/jzus.B1000265](https://doi.org/10.1631/jzus.B1000265) 2011.
- 376 Mansour, M. F., Morgenstern, N. R., and Martin, C. D.: Expected damage from displacement of slow-
377 moving slides. Landslides, 8(1), 117-131. [https://doi: 10.1007/s10346-010-0227-7](https://doi.org/10.1007/s10346-010-0227-7) 2011.
- 378 Pal, R.: Entropy Production in Pipeline Flow of Dispersions of Water in Oil. Entropy, 16(8), 4648-4661.
379 [https://doi: 10.3390/e16084648](https://doi.org/10.3390/e16084648) 2014.
- 380 Qiu, D., Niu, R., ZhaoYannan, and Wu, X.: Risk Zoning of Earthquake-Induced Landslides Based on
381 Slope Units:A Case Study on Lushan Earthquake. Journal of Jilin University, 45(5), 1470-1478.
382 [https://doi: 10.13278/j.cnki.jjuese.201505201](https://doi.org/10.13278/j.cnki.jjuese.201505201) 2015.
- 383 Rafiq, L., and Blaschke, T.: Disaster risk and vulnerability in Pakistan at a district level. Geomatics
384 Natural Hazards & Risk, 3(4), 324-341. [https://doi: 10.1080/19475705.2011.626083](https://doi.org/10.1080/19475705.2011.626083) 2012.
- 385 Ray, P. K. C., Dimri, S., Lakhera, R. C., and Sati, S.: Fuzzy-based method for landslide hazard assessment
386 in active seismic zone of Himalaya. Landslides, 4(2), 101. [https://doi: 10.1007/s10346-006-0068-6](https://doi.org/10.1007/s10346-006-0068-6) 2007.
- 387 Sari, D. A. P., Innaqa, S., and Safrilah. Hazard, Vulnerability and Capacity Mapping for Landslides Risk
388 Analysis using Geographic Information System (GIS). 209(1), 012106. [https://doi: 10.1088/1757-
389 899X/209/1/012106](https://doi.org/10.1088/1757-899X/209/1/012106) 2017.
- 390 Sarkar, S., and Gupta, P. K.: Techniques for Landslide Hazard Zonation – Application to Srinagar-
391 Rudraprayag Area of Gar. Journal of the Geological Society of India, 65(2), 217-230. 2005.
- 392 Shi, S.: Risk Analysis for Pipeline Construction about Third Party Damage Based on Triangular Fuzzy
393 Number and Fault Tree Theory. Journal of Chongqing University of Science & Technology. 2011.
- 394 Su, G., and Deng, F.: On the Improving Backpropagation Algorithms of the Neural Networks Based on
395 MATLAB Language:A Review. Bulletin of Science & Technology. 2003.
- 396 Wang, P., Xu, Z., Bai, M., Du, Y., Mu, S., Wang, D., and Yang, Y.: Landslide Risk Assessment Expert
397 System Along the Oil and Gas Pipeline Routes. Advanced Materials Research, 418-420, 1553-1559.
398 [https://doi: 10.4028/www.scientific.net/AMR.418-420.1553](https://doi.org/10.4028/www.scientific.net/AMR.418-420.1553) 2012.



- 399 Wu, T. H., Tang, W. H., and Einstein, H. H. (1996). Landslides: investigation and mitigation. chapter 6 -
400 landslide hazard and risk assessment.
- 401 Xiang, L. Z., Cui, P., Zhang, J. Q., Huang, D. C., Fang, H., and Zhou, X. J.: Triggering factors
402 susceptibility of earthquake-induced collapses and landslides in Wenchuan County. *Journal of Sichuan*
403 *University*, 42(5), 105-112. 2010.
- 404 Xin, Y., Chong, X. U., and Dai, F. C.: Contribution of strata lithology and slope gradient to landslides
405 triggered by Wenchuan Ms 8 earthquake, Sichuan, China. *Geological Bulletin of China*, 28(8), 1156-1162.
406 2009.
- 407 Ye, C., Jiang, H., Yao, A., Xia, Q., and Zhao, X.: Study on risk controlling method of third party
408 construction damage on oil and gas pipeline. *Journal of Safety Science & Technology*, 9(8), 140-145.
409 2013.
- 410 Yun, L., and Kang, L.: Reliability Analysis of High Pressure Buried Pipeline under Landslide. *Applied*
411 *Mechanics & Materials*, 501-504, 1081-1086. [https://doi: 10.4028/www.scientific.net/AMM.501-](https://doi.org/10.4028/www.scientific.net/AMM.501-504.1081)
412 [504.1081](https://doi.org/10.4028/www.scientific.net/AMM.501-504.1081) 2014.
- 413 Zhang, Y., Shi, J., Gan, J., and Liu, C.: Analysis of Distribution Characteristics and Influencing Factors
414 of Secondary Geohazards in Guangyuan City—Taking Chaotian District as an Example. *Journal of*
415 *Catastrophology*, 26(1), 75-79. [https://doi: 10.1007/s12182-011-0118-0](https://doi.org/10.1007/s12182-011-0118-0) 2011.
- 416 Zheng, J. Y., Zhang, B. J., Liu, P. F., and Wu, L. L.: Failure analysis and safety evaluation of buried
417 pipeline due to deflection of landslide process. *Engineering Failure Analysis*, 25(4), 156-168. [https://doi:](https://doi.org/10.1016/j.engfailanal.2012.05.011)
418 [10.1016/j.engfailanal.2012.05.011](https://doi.org/10.1016/j.engfailanal.2012.05.011) 2012.
- 419



420 **List of tables and figures**

421 **Table 1** Indicators of landslide hazard assessment and pipeline vulnerability assessment

422 **Table 2** Entropy weight of evaluation index

423 **Table 3** Number and area of slopes of four hazard grade

424 **Table 4** Number and distances of pipeline of four vulnerability grade

425 **Table 5** Number and distances of pipeline of four risk grade

426 **Table 6** Description of pipeline risk level

427

428 **Figure 1** Landslide location map of the study area

429 **Figure 2** All slope units (a) and pipeline section (b) in the study area

430 **Figure 3** The frequency distribution of each factor in the landslide location. Maps (a), (b), (c), (d), (e),

431 (f), (g), and (h) represent the elevation, slope, aspect, height difference, TPC, NVI, MAP, and distance

432 from the fault, respectively

433 **Figure 4** Landslide hazard map of study area

434 **Figure 5** Pipeline vulnerability map of study area

435 **Figure 6** Pipeline risk map of study area

436



437
 438
 439
 440
 441
 442
 443
 444
 445

Table 1

	Factor	Indicators
Landslide hazard index	Landform	Elevation
		Slope
		Aspect
		Height Difference
	Land cover	Topographic profile curvature (TPC)
		NDVI
	Geology	NDWI
		Lithology
	Precipitation	Distance from the fault
		Mean annual precipitation (MAP)
Pipeline vulnerability index	Precipitation	Coefficient of variation of annual rainfall (CVAR)
		Defect Density
	Pipe Body	Depth
		Thickness
		Pressure
		Materials
	Spatial relationship between pipeline and landslide	Diameter
		Media
		Position
		Angle

446
 447
 448



449
450
451
452
453
454
455
456
457
458
459
460
461
462
463

Table 2

	Depth	Angle	Defect Density	Thickness	Position
Weight	0.010007	0.101553	0.678851	0.154322	0.055266
Entropy	0.997322	0.97282	0.818308	0.958696	0.985208

464
465



466

Table 3

Landslide hazard	Number of slopes	Percentage	Area (km ²)	Percentage
Low (I)	33	10.48%	32.63	8.76%
Medium (II)	62	19.68%	65.53	17.60%
High (III)	112	35.56%	123.55	33.18%
Extremely high (IV)	108	34.29%	150.65	40.46%
Total	315	100%	372.36	100%

467

468



469

Table 4

Pipeline vulnerability	Number of pipelines	Percentage	Area (km ²)	Percentage
Low (I)	120	66.66%	50.417	62.06%
Medium (II)	37	20.56%	20.888	25.72%
High (III)	22	12.22%	9.833	12.11%
Extremely (IV)	1	0.56%	0.087	0.11%
Total	180	100%	81.225	100%

470

471



472

Table 5

Pipeline risk	Number of pipelines	Percentage	Area (km ²)	Percentage
Low (I)	37	20.56%	14.469	17.81%
Medium (II)	106	58.89%	50.757	62.49%
High (III)	33	18.33%	13.461	16.57%
Extremely (IV)	4	2.22%	2.538	3.13%
Total	180	100%	81.225	100%

473

474



475

Table 6

Pipeline risk	landslides hazard	Vulnerability	Risk	Control measures
Low (I)	The landslide won't happen under ordinary conditions, but it will occur when strong earthquake, long continuous rain or extremely heavy rain happened.	The pipes in low risk areas have no any defects and buried very deep. Meanwhile, they are far away from the area affected by landslide.	Landslides have no obvious damage to the pipes, and few threats to pipes' safety.	Regular Inspection
Medium (II)	Small landslide mainly occur, and no sign of deformation. But through analyzing geological structure, topography and landform, there is a tendency of landslide.	The pipes in risk areas have almost no faults and buried deep. However, under bad condition, the landslide may also affect the pipes' safety.	The landslide may make the pipes exposed or deformation.	simple monitoring
High (III)	Landslides are most in medium-model and little-model, and they are in deformation, or have obvious deformation recently, such as obvious cracks, subsidence or tympanites on the landslide and even shear.	The pipeline has defects, and buried shallow. Once landslides occurred in the pipeline area, pipes' safety will be threatened	The safety of pipeline will be threatened and may suffer from pipe suspension, floating, and damage etc. Therefore it will contribute to a small amount of medium leakage. Fortunately, the pipe can be welded or repaired.	Main monitoring
Extremely high (IV)	Large or huge landslide is common in the area with extremely high risk, which is changing or has experienced obvious deformation recently with visible cracks.	The pipelines are subject to dangers at any time as the pipelines within the area prone to landslide have been spotted with many defects or much damage.	There are great threats, for example pipeline rupture or break and may lead to considerable leakage of media or serious deformation even transportation failure.	Prevention and control measures shall be taken in a short time

476

477

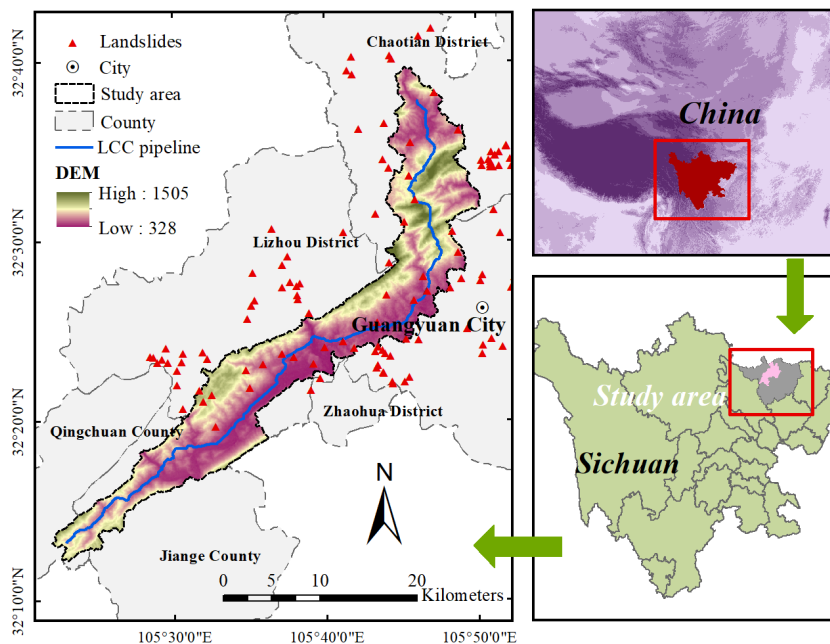
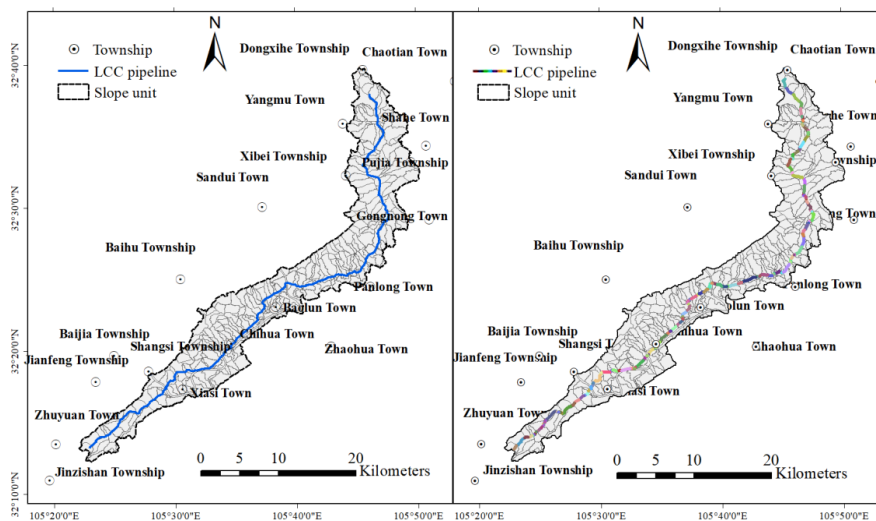


Figure 1

478
479
480
481

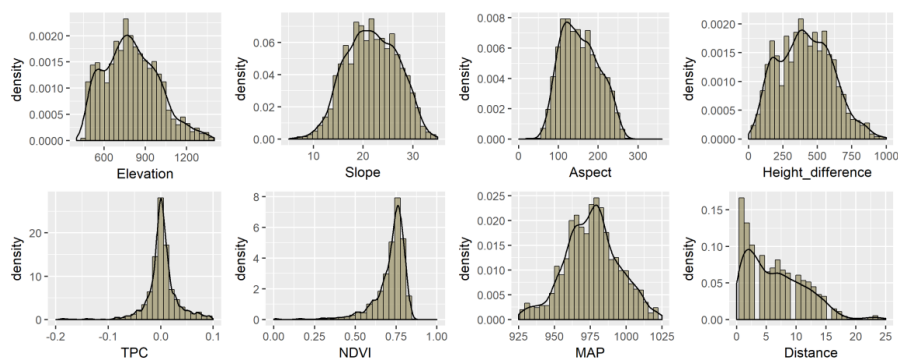


482

483

Figure 2

484



485

486

487

Figure 3

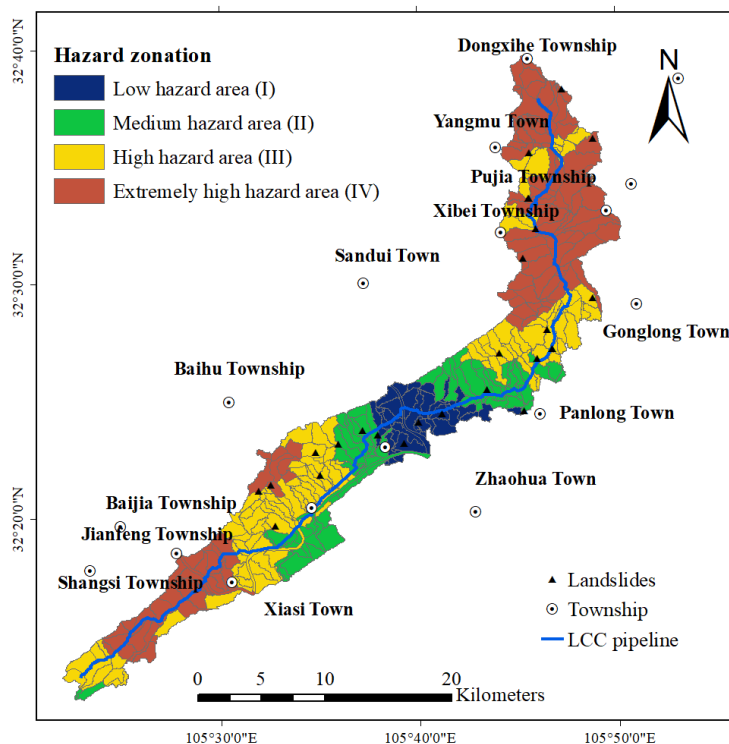


Figure 4

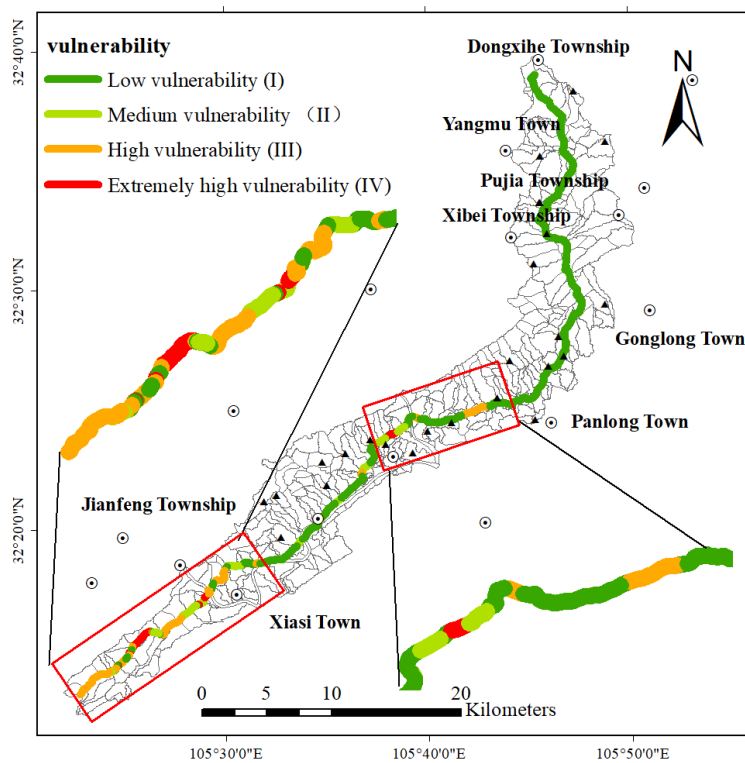
488

489

490

491

492

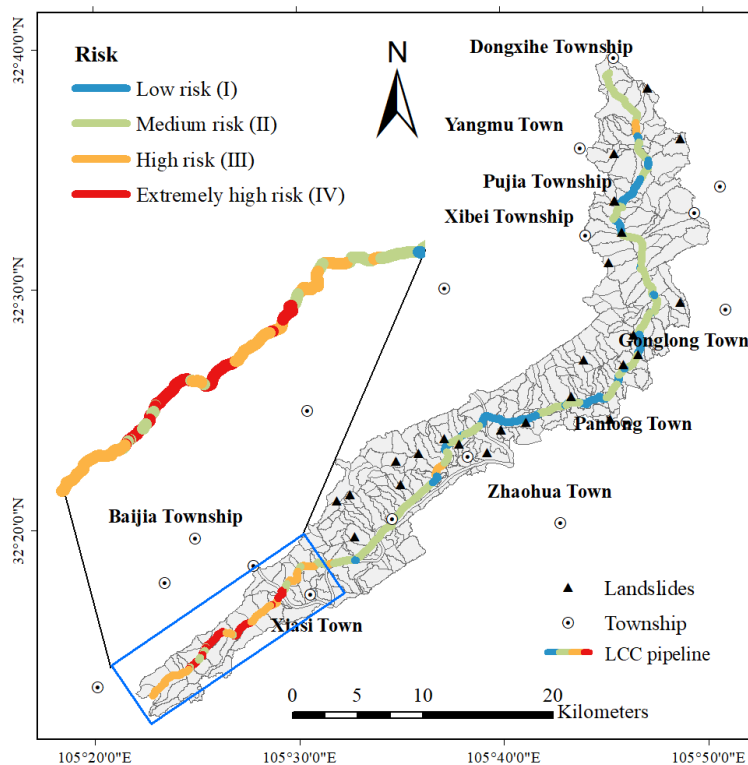


493

494

495

Figure 5



496

497

498

499

Figure 6



500 **Appendix 1 Classification of landslide hazard grade corresponding to different intervals**

Factor	Indicators	Interval	Hazard degree monotonicity	Hazard level
Landform	Elevation	[1000 , Highest]	Decreasing	Low hazard(I)
		[Lowest , 600)	Increasing	Medium hazard(II)
		[800 , 1000)	Decreasing	High hazard(III)
		[600 , 700) ∪ [700 , 800)	Increasing, Decreasing	Extremely high hazard(IV)
	Slope	[60 , 90)	Decreasing	Low hazard(I)
		[0 , 15)	Increasing	Medium hazard(II)
		[30 , 60)	Decreasing	High hazard(III)
		[15 , 20) ∪ [20 , 30)	Increasing, Decreasing	Extremely high hazard(IV)
	Aspect	[0 , 45) ∪ [270 , 360)	Increasing, Decreasing	Low hazard(I)
		[225 , 270) ∪ [45 , 90)	Decreasing, Increasing	Medium hazard(II)
		[90 , 135) ∪ [180 , 225)	Increasing, Decreasing	High hazard(III)
		[135 , 157.5) ∪ [157.5 , 180)	Increasing, Decreasing	Extremely high hazard(IV)
Land cover	Height difference	[Lowest , 100)	Increasing	Low hazard(I)
		[900 , Highest] ∪ [100 , 200)	Decreasing, Increasing	Medium hazard(II)
		[600 , 900) ∪ [200 , 300)	Decreasing, Increasing	High hazard(III)
		[300 , 450) ∪ [450 , 600)	Increasing, Decreasing	Extremely high hazard(IV)
	topographic profile curvature	[Lowest , -0.025)	Increasing	Low hazard(I)
		[0.025 , Highest]	Decreasing	Medium hazard(II)
		[-0.025 , -0.01) ∪ [0.01 , 0.025)	Increasing, Decreasing	High hazard(III)
		[-0.01 , 0) ∪ [0 , 0.01)	Increasing, Decreasing	Extremely high hazard(IV)
	NDVI	[-1,0)	Increasing	Low hazard(I)
		[0,0.6) ∪ [0.9,1]	Increasing, Decreasing	Medium hazard(II)
		[0.6,0.7) ∪ [0.8,0.9)	Increasing, Decreasing	High hazard(III)
		[0.7,0.75) ∪ [0.75,0.8)	Increasing, Decreasing	Extremely high hazard(IV)
Precipitation	Mean annual precipitation	[1100 , Highest)	Decreasing	Low hazard(I)
		[Lowest , 960)	Increasing	Medium hazard(II)
		[990 , 1100)	Decreasing	High hazard(III)
		[960 , 975) ∪ [975 , 990)	Increasing, Decreasing	Extremely high hazard(IV)
Geology	Distance from the fault	[20 , Highest]	Decreasing	Low hazard(I)
		[15 , 20)	Decreasing	Medium hazard(II)
		[5 , 15)	Decreasing	High hazard(III)
		[0 , 5)	Decreasing	Extremely high hazard(IV)



Appendix 2 Standard training sample matrix and standard test sample matrix

Sample type	ID	Input										Output
		Aspect	Slope	Elevation	NDVI	MAP	Height Difference	TPC	Distance	Lithology		
Training sample	1	0.2	89.9	438	-1	908.1	33	-0.582	25	1	0	
	50	35.2	82.8	453	0	912.2	79	-0.456	23.47	1	0.06	
	100	297.1	75.7	469	0.88	916.3	115	-0.33	21.9	1	0.12	
	150	329.3	67.6	485	0.95	920.4	167	-0.168	20.34	1	0.19	
	200	359.5	60	499	1	924.9	200	0.628	18.77	1	0.25	
	250	68.4	3.8	1293	0.73	930.4	1097	0.486	17.21	2	0.31	
	300	89.3	8.2	1206	0.65	938	1039	0.326	15.64	2	0.37	
	350	246	12	1102	0.56	943.6	977	0.183	14.08	2	0.44	
	400	269.3	15	1002	0.5	949.8	902	-0.142	12.52	2	0.5	
	450	113.4	52.9	952	0.46	960.6	848	-0.018	10.95	3	0.56	
	500	134.8	46.3	905	0.4	972.6	757	-0.012	9.39	3	0.62	
	1	27.2	72.3	458	0.8	911.6	59	-0.544	25	1	0	
	2	28.5	71.6	468	0.81	914.3	74	-0.453	23.69	1	0.06	
3	31.5	69.5	488	0.85	915.8	86	-0.381	22.37	1	0.11		
4	37.8	66.2	490	0.86	917.1	100	-0.228	21.06	1	0.16		
5	38.6	62.1	497	0.86	919.1	152	-0.03	19.74	1	0.22		
6	56.1	4.4	1141	0.7	934.2	939	0.439	18.43	2	0.27		
7	57.3	6.6	1240	0.68	939.6	941	0.429	17.11	2	0.32		
8	65.3	9.8	1257	0.66	945.1	1124	0.413	15.79	2	0.37		
9	68.2	11	1290	0.56	948.8	1135	0.318	14.48	2	0.43		
10	74.7	11.9	1382	0.53	949.9	1146	0.148	13.16	2	0.48		
11	92.4	30.4	848	0.47	963.4	613	-0.019	11.85	3	0.53		
12	92.7	31.8	853	0.45	970.5	683	-0.016	10.53	3	0.58		
13	101.9	44.7	900	0.45	980.5	737	-0.015	9.22	3	0.64		
Test sample												



14	110.1	50.9	917	0.35	987	817	-0.015	7.9	3	0.69
15	115.6	57.5	933	0.32	994.2	835	-0.015	6.58	3	0.74
16	140.6	15.6	502	0.14	1001.5	245	0.019	5.27	4	0.79
17	155.4	20	626	0.14	1002.3	256	0.008	3.95	4	0.85
18	157.1	24.8	690	0.08	1010.6	293	0.007	2.64	4	0.9
19	177.6	27.3	765	0.06	1012.7	392	0.004	1.32	4	0.95
20	178.3	29.6	795	0.04	1022.7	446	0.001	0	4	1



505

Appendix 3 Test error of LM-BP neural network

Number	Expected value	network output	error
1	0	0.0006	0.0006
2	0.06	0.0548	-0.0052
3	0.11	0.1113	0.0013
4	0.16	0.1699	0.0099
5	0.22	0.2302	0.0102
6	0.27	0.2614	-0.0086
7	0.32	0.315	-0.005
8	0.37	0.3697	-0.0003
9	0.43	0.4266	-0.0034
10	0.48	0.4899	0.0099
11	0.53	0.5153	-0.0147
12	0.58	0.5765	-0.0035
13	0.64	0.6405	0.0005
14	0.69	0.701	0.011
15	0.74	0.7523	0.0123
16	0.79	0.8094	0.0194
17	0.85	0.8616	0.0116
18	0.9	0.9155	0.0155
19	0.95	0.9675	0.0175
20	1	1.0173	0.0173

506



Appendix 4 Coordinates of the center line and ancillary facilities of the pipeline

Point number	Previous point	Material	Diameter (mm)	Pressure	Depth (m)	Coordinate			elevation
						X	Y	H	
Marker peg									
GDI.421	GD1.420	Steel	168	high	--	--576.265	--4357.849	503.877	--
GDI.422	GD1.421	Steel	168	high	2.2	--572.111	--4352.109	504.235	502.035
GDI.423	GD1.422	Steel	168	high	1.9	--571.837	--4336.010	503.866	501.966
GDI.424	GD1.423	Steel	168	high	2.1	--571.538	--4319.679	503.694	501.594
GDI.425	GD1.424	Steel	168	high	2.1	--571.093	--4308.825	503.510	501.410
Detective pole K566					2.0	--570.718	--4288.141	503.733	501.733
					--	--575.536	--4284.069	503.494	--
GDI.426	GD1.425	Steel	168	high	2.3	--570.603	--4275.147	503.998	501.698
Mileage peg K566+200					--	--574.641	--4258.41	503.224	--
GDI.427	GD1.426	Steel	168	high	2.0	--570.222	--4258.593	503.710	501.710
GDI.428	GD1.427	Steel	168	high	1.6	--570.090	--4247.642	503.283	501.683
GDI.429	GD1.428	Steel	168	high	2.3	--569.458	--4216.618	502.468	500.168
GDI.430	GD1.429	Steel	168	high	2.9	--569.043	--4208.558	504.055	501.155



Appendix 5 Internal detection data of pipeline

FID	Pipe number	distance(m)	Feature type	Remarks	Length (mm)	thickness (mm)
1	10	6.408	Pipe segment	Spiral weld	652	11.1
2	20	7.060	Pipe segment	--	1178	--
3	20	7.648	Fixed punctuation point	Valve centerline	--	--
4	20	7.650	Valve	centerline	--	--
5	30	8.238	Pipe segment	Spiral weld	768	11.1
6	40	9.006	Pipe segment	--	2184	--
7	40	10.100	Globular tee	centerline	--	--
8	50	11.190	Pipe segment	Spiral weld	1700	11.1
9	50	11.445	Pit	--	548	11.1
10	60	12.890	Pipe segment	Straight weld	2342	13.6
11	60	12.890	Wall thickness variation	from 11.1mmto 13.6mm	--	--
13	70	15.232	Pipe segment	Spiral weld	1999	11.1
14	70	15.232	Wall thickness variation	from 13.6mmto 11.1mm	--	--
15	80	17.231	Pipe segment	Straight weld	2352	13.4
16	80	17.231	Wall thickness variation	from 11.1mmto 13.4mm	--	--
18	90	19.583	Pipe segment	Spiral weld	11557	11.1
19	90	19.583	Wall thickness variation	from 13.4mmto 11.1mm	--	--
20	90	28.060	Attachments	--	598	11.1
21	100	31.140	Pipe segment	--	991	--
22	100	31.580	Flange	centerline	--	--
23	110	32.131	Pipe segment	Spiral weld	11660	11.1
24	120	43.791	Pipe segment	Spiral weld	5536	11.1
25	130	49.327	Pipe segment	Straight weld	2213	16.2
26	130	49.327	Wall thickness variation	from 11.1mmto 16.2mm	--	--



28	140	51.540	Pipe segment	Spiral weld	5608	11.1
29	140	51.540	Wall thickness variation	from 16.2mm to 11.1mm	--	--
30	150	57.148	Pipe segment	Spiral weld	9432	11.1



527 **Appendix 6 Core Code of Pipeline Defect Point Coordinate Calculating Program**

```
528 using System;
529 using System.Collections.Generic;
530 using System.ComponentModel;
531 using System.Data;
532 using System.Drawing;
533 using System.Linq;
534 using System.Text;
535 using System.Threading.Tasks;
536 using System.Windows.Forms;
537 using System.IO;
538 private void button10_Click(object sender, EventArgs e)
539 {
540     double x1 = 0, y1 = 0, z1 = 0, x2 = 0, y2 = 0, z2 = 0, d1 = 0, d2 = 0, h1 = 0, h2 = 0;
541     double l = Convert.ToDouble(textBox9.Text);
542     double f = 0, nl = Convert.ToDouble(textBox7.Text);
543     string[] SplitTxt = textBox2.Text.Split(',');
544     for (long i = 0; i < SplitTxt.Length - 9; i += 5)
545     {
546         d1 = Convert.ToDouble(SplitTxt[i + 1]);
547         x1 = Convert.ToDouble(SplitTxt[i + 2]);
548         y1 = Convert.ToDouble(SplitTxt[i + 3]);
549         z1 = Convert.ToDouble(SplitTxt[i + 4]);
550         d2 = Convert.ToDouble(SplitTxt[i + 6]);
551         x2 = Convert.ToDouble(SplitTxt[i + 7]);
552         y2 = Convert.ToDouble(SplitTxt[i + 8]);
553         z2 = Convert.ToDouble(SplitTxt[i + 9]);
554         h1 = z1 - d1;
555         h2 = z2 - d2;
556         l += Math.Sqrt((x1 - x2) * (x1 - x2) + (y1 - y2) * (y1 - y2) + (h1 - h2) * (h1 - h2));
557     }
558     textBox8.Text = l.ToString();
559     f = (nl - l) / nl;
560     ff = f;
561     textBox5.Text = Convert.ToDouble(f).ToString("P");
562 }
563 private void button9_Click(object sender, EventArgs e)
564 {
565     double f1 = ff;
566     double l1 = 0;
567     string zb = ""; string[] SplitTxt = textBox3.Text.Split(',');
568     for (long i = 0; i < SplitTxt.Length - 1; i += 2)
569     {
570         l1 = Convert.ToDouble(SplitTxt[i + 1]);
```



```
571         l1 += (-ff) * l1;
572         double x1 = 0, y1 = 0, z1 = 0, x2 = 0, y2 = 0, z2 = 0, d1 = 0, d2 = 0, h1 = 0, h2 = 0, l0=0,l2=0;
573         double l = Convert.ToDouble(textBox9.Text);
574         double x = 0, y = 0, h = 0;
575         string[] SplitTxt1 = textBox2.Text.Split(',');
576         for (long j = 0; j < SplitTxt1.Length - 9; j += 5)
577             {
578                 d1 = Convert.ToDouble(SplitTxt1[j + 1]);
579                 x1 = Convert.ToDouble(SplitTxt1[j + 2]);
580                 y1 = Convert.ToDouble(SplitTxt1[j + 3]);
581                 z1 = Convert.ToDouble(SplitTxt1[j + 4]);
582                 d2 = Convert.ToDouble(SplitTxt1[j + 6]);
583                 x2 = Convert.ToDouble(SplitTxt1[j + 7]);
584                 y2 = Convert.ToDouble(SplitTxt1[j + 8]);
585                 z2 = Convert.ToDouble(SplitTxt1[j + 9]);
586                 h1 = z1 - d1; h2 = z2 - d2;
587                 l0= Math.Sqrt((x1 - x2) * (x1 - x2) + (y1 - y2) * (y1 - y2) + (h1 - h2) * (h1 - h2));
588                 l = 1 + l0;
589                 if (l - l1 < 0)
590                     {
591                         ;
592                     }
593                 else if (l - l1 > 0)
594                     {
595                         l2 = l0 - (l - l1);
596                         x = x1 + (x2 - x1) * l2 / l0;
597                         y = y1 + (y2 - y1) * l2 / l0;
598                         h = h1 + (h2 - h1) * l2 / l0;
599                         string xx, yy, hh, v;
600                         v = SplitTxt1[i];
601                         xx = Convert.ToDouble(x).ToString();
602                         yy = Convert.ToDouble(y).ToString();
603                         hh = Convert.ToDouble(h).ToString();
604                         zb +=v + ","+ xx + ","+ yy + ","+ hh +",\n";
605                         break;
606                     }
607             }
608     }
609     textBox6.Text = zb;
610 }
```



611

Appendix 7 Pipeline Landslide Risk Assessment Results

Fid	Start	Terminus	Hazard	Hazard level	Vulnerability	Vulnerability level	Risk	Risk level
1	K558	K559+446	0.874	IV	0.168	I	0.147	II
2	K559+446	K563+718	0.874	IV	0.178	I	0.156	II
3	K563+718	K564+883	0.932	IV	0.143	I	0.133	II
4	K564+883	K566+90	0.943	IV	0.149	I	0.141	II
5	K566+90	K567+117	0.943	IV	0.280	II	0.264	III
6	K567+117	K567+224	0.766	IV	0.095	I	0.073	I
7	K567+224	K567+384	0.729	III	0.117	I	0.085	II
8	K567+384	K567+674	0.729	III	0.079	I	0.058	I
9	K567+674	K567+782	0.729	III	0.141	I	0.103	II
10	K567+782	K567+846	0.729	III	0.066	I	0.048	I
11	K567+846	K567+904	0.729	III	0.097	I	0.071	I
12	K568+904	K568+197	0.722	III	0.154	I	0.111	II
13	K568+197	K568+430	0.763	IV	0.144	I	0.110	II
14	K569+430	K569+419	0.739	III	0.186	I	0.137	II
15	K569+419	K569+443	0.739	III	0.141	I	0.104	II
16	K569+443	K569+467	0.739	III	0.107	I	0.079	II
17	K569+467	K569+578	0.739	III	0.121	I	0.089	II
18	K569+578	K569+920	0.739	III	0.107	I	0.079	II
19	K571+920	K571+123	0.736	III	0.127	I	0.093	II
20	K571+123	K571+982	0.799	IV	0.109	I	0.087	II
21	K572+982	K572+729	0.753	IV	0.090	I	0.068	I
22	K573+729	K573+548	0.802	IV	0.094	I	0.075	I
23	K574+548	K574+249	0.805	IV	0.084	I	0.068	I
24	K574+249	K574+525	0.805	IV	0.150	I	0.121	II
25	K575+525	K575+538	0.805	IV	0.115	I	0.093	II
26	K575+538	K575+600	0.805	IV	0.157	I	0.126	II
27	K576+600	K576+737	0.816	IV	0.108	I	0.088	II
28	K577+737	K577+120	0.889	IV	0.089	I	0.079	I
29	K577+120	K577+146	0.889	IV	0.094	I	0.084	I
30	K577+146	K577+187	0.889	IV	0.169	I	0.150	II
31	K578+187	K578+571	0.889	IV	0.118	I	0.105	II
32	K578+571	K578+608	0.889	IV	0.095	I	0.084	I
33	K579+608	K579+624	0.853	IV	0.133	I	0.113	II
34	K580+624	K580+582	0.871	IV	0.156	I	0.136	II
35	K581+582	K581+43	0.871	IV	0.097	I	0.084	I
36	K581+43	K581+273	0.871	IV	0.143	I	0.125	II
37	K581+273	K581+536	0.880	IV	0.125	I	0.110	II
38	K581+536	K581+659	0.872	IV	0.154	I	0.134	II
39	K582+659	K582+263	0.830	IV	0.152	I	0.126	II
40	K582+263	K582+437	0.830	IV	0.116	I	0.096	II
41	K583+437	K583+512	0.830	IV	0.152	I	0.126	II
42	K583+512	K583+693	0.798	IV	0.105	I	0.084	II
43	K583+693	K583+720	0.740	III	0.113	I	0.084	II
44	K585+720	K585+55	0.740	III	0.178	I	0.132	II
45	K585+55	K585+101	0.668	III	0.196	I	0.131	II
46	K585+101	K585+370	0.668	III	0.178	I	0.119	II
47	K585+370	K585+634	0.696	III	0.190	I	0.132	II
48	K585+634	K585+734	0.668	III	0.116	I	0.077	II



49	K585+734	K585+908	0.627	III	0.198	I	0.124	II
50	K585+908	K585+949	0.627	III	0.168	I	0.105	II
51	K586+949	K586+782	0.627	III	0.173	I	0.108	II
52	K586+782	K586+805	0.627	III	0.117	I	0.073	II
53	K587+805	K587+364	0.627	III	0.171	I	0.107	II
54	K587+364	K587+498	0.618	III	0.078	I	0.048	I
55	K587+498	K587+794	0.618	III	0.107	I	0.066	I
56	K589+794	K589+251	0.618	III	0.102	I	0.063	I
57	K590+251	K590+757	0.618	III	0.172	I	0.106	II
58	K590+757	K590+780	0.556	III	0.153	I	0.085	II
59	K590+780	K590+812	0.556	III	0.123	I	0.068	II
60	K591+812	K591+500	0.555	III	0.135	I	0.075	II
61	K591+500	K591+946	0.555	III	0.087	I	0.048	I
62	K592+946	K592+259	0.555	III	0.107	I	0.059	I
63	K593+259	K593+631	0.517	III	0.152	I	0.079	II
64	K593+631	K593+912	0.374	II	0.153	I	0.057	II
65	K594+912	K594+993	0.374	II	0.150	I	0.056	II
66	K595+993	K595+203	0.374	II	0.076	I	0.028	I
67	K595+203	K595+261	0.359	II	0.114	I	0.041	I
68	K595+261	K595+383	0.359	II	0.099	I	0.036	I
69	K596+383	K596+383	0.412	II	0.278	II	0.115	II
70	K596+383	K596+429	0.412	II	0.107	I	0.044	I
71	K597+429	K597+62	0.359	II	0.121	I	0.043	I
72	K597+62	K597+200	0.412	II	0.158	I	0.065	II
73	K597+200	K597+345	0.412	II	0.133	I	0.055	I
74	K597+345	K597+680	0.412	II	0.273	II	0.112	II
75	K599+680	K599+376	0.321	II	0.461	II	0.148	II
76	K599+376	K599+693	0.211	I	0.105	I	0.022	I
77	K600+693	K600+188	0.211	I	0.179	I	0.038	I
78	K600+188	K600+353	0.106	I	0.172	I	0.018	I
79	K601+353	K601+369	0.106	I	0.264	II	0.028	I
80	K602+369	K602+495	0.099	I	0.190	I	0.019	I
81	K603+495	K603+131	0.067	I	0.436	II	0.029	I
82	K603+131	K603+551	0.099	I	0.144	I	0.014	I
83	K604+551	K604+321	0.104	I	0.253	II	0.026	I
84	K604+321	K604+976	0.099	I	0.102	I	0.010	I
85	K605+976	K605+735	0.178	I	0.372	II	0.066	II
86	K606+735	K606+368	0.236	I	0.637	III	0.150	II
87	K606+368	K606+838	0.236	I	0.127	I	0.030	I
88	K607+838	K607+596	0.323	II	0.407	II	0.131	II
89	K608+596	K608+20	0.323	II	0.163	I	0.053	II
90	K608+20	K608+287	0.323	II	0.145	I	0.047	I
91	K608+287	K608+546	0.346	II	0.084	I	0.029	I
92	K608+546	K608+583	0.406	II	0.215	I	0.087	II
93	K608+583	K608+835	0.406	II	0.291	II	0.118	II
94	K609+835	K609+565	0.442	II	0.279	II	0.123	II
95	K610+565	K610+564	0.442	II	0.403	II	0.178	II
96	K610+564	K610+945	0.442	II	0.453	II	0.200	II
97	K611+945	K611+89	0.482	II	0.117	I	0.056	I
98	K611+89	K611+691	0.501	III	0.138	I	0.069	II
99	K612+691	K612+413	0.501	III	0.175	I	0.088	II



100	K613+413	K613+269	0.501	III	0.163	I	0.082	II
101	K613+269	K613+442	0.502	III	0.166	I	0.083	II
102	K614+442	K614+83	0.502	III	0.354	II	0.178	II
103	K614+83	K614+980	0.502	III	0.263	II	0.132	II
104	K615+980	K615+218	0.601	III	0.153	I	0.092	II
105	K615+218	K615+388	0.601	III	0.143	I	0.086	II
106	K616+388	K616+87	0.635	III	0.126	I	0.080	II
107	K616+87	K616+300	0.556	III	0.144	I	0.080	II
108	K616+300	K616+460	0.505	III	0.269	II	0.136	II
109	K617+460	K617+715	0.505	III	0.172	I	0.087	II
110	K617+715	K617+827	0.505	III	0.255	II	0.129	II
111	K618+827	K618+28	0.556	III	0.170	I	0.095	II
112	K618+28	K618+687	0.556	III	0.313	II	0.174	II
113	K620+687	K620+78	0.556	III	0.188	I	0.105	II
114	K620+78	K620+298	0.425	II	0.196	I	0.083	II
115	K621+298	K621+509	0.576	III	0.223	I	0.128	II
116	K621+509	K621+611	0.425	II	0.107	I	0.045	I
117	K622+611	K622+10	0.425	II	0.262	II	0.111	II
118	K622+10	K622+86	0.425	II	0.122	I	0.052	I
119	K622+86	K622+539	0.693	III	0.178	I	0.123	II
120	K622+539	K622+897	0.634	III	0.549	III	0.348	III
121	K623+897	K623+36	0.634	III	0.535	III	0.339	III
122	K623+36	K623+794	0.693	III	0.145	I	0.100	II
123	K624+794	K624+866	0.693	III	0.310	II	0.215	II
124	K625+866	K625+242	0.796	IV	0.137	I	0.109	II
125	K627+242	K627+60	0.859	IV	0.452	II	0.388	III
126	K627+60	K627+162	0.859	IV	0.193	I	0.166	II
127	K627+162	K627+313	0.859	IV	0.166	I	0.143	II
128	K627+313	K627+700	0.783	IV	0.167	I	0.131	II
129	K628+700	K628+146	0.908	IV	0.501	III	0.455	III
130	K628+146	K628+196	0.908	IV	0.139	I	0.126	II
131	K628+196	K628+610	0.908	IV	0.631	III	0.573	IV
132	K629+610	K629+355	0.787	IV	0.369	II	0.290	III
133	K629+355	K629+525	0.787	IV	0.729	III	0.574	IV
134	K629+525	K629+570	0.787	IV	0.252	II	0.198	II
135	K629+570	K629+620	0.787	IV	0.465	II	0.366	III
136	K630+620	K630+348	0.787	IV	0.286	II	0.225	II
137	K630+348	K630+956	0.892	IV	0.389	II	0.347	III
138	K631+956	K631+116	0.886	IV	0.423	II	0.375	III
139	K631+116	K631+528	0.805	IV	0.513	III	0.413	III
140	K633+528	K633+435	0.805	IV	0.568	III	0.457	III
141	K635+435	K635+302	0.933	IV	0.625	III	0.583	IV
142	K635+302	K635+326	0.884	IV	0.611	III	0.540	III
143	K635+326	K635+359	0.884	IV	0.441	II	0.390	III
144	K635+359	K635+368	0.884	IV	0.194	I	0.171	II
145	K635+368	K635+530	0.884	IV	0.374	II	0.331	III
146	K635+530	K635+604	0.884	IV	0.307	II	0.271	III
147	K635+604	K635+850	0.805	IV	0.377	II	0.303	III
148	K635+850	K635+943	0.805	IV	0.234	I	0.188	II
149	K635+943	K635+972	0.805	IV	0.139	I	0.112	II
150	K635+972	K635+974	0.805	IV	0.121	I	0.097	II



151	K635+974	K635+990	0.805	IV	0.138	I	0.111	II
152	K636+990	K636+152	0.933	IV	0.598	III	0.558	III
153	K636+152	K636+159	0.933	IV	0.157	I	0.146	II
154	K636+159	K636+320	0.884	IV	0.579	III	0.512	III
155	K636+320	K636+427	0.884	IV	0.166	I	0.147	II
156	K636+427	K636+517	0.884	IV	0.124	I	0.110	II
157	K636+517	K636+806	0.834	IV	0.663	III	0.553	III
158	K636+806	K636+893	0.834	IV	0.794	IV	0.662	IV
159	K637+893	K637+57	0.834	IV	0.519	III	0.433	III
160	K637+57	K637+109	0.834	IV	0.542	III	0.452	III
161	K637+109	K637+181	0.834	IV	0.111	I	0.093	II
162	K637+181	K637+332	0.834	IV	0.127	I	0.106	II
163	K638+332	K638+87	0.834	IV	0.608	III	0.507	III
164	K638+87	K638+140	0.834	IV	0.157	I	0.131	II
165	K638+140	K638+193	0.767	IV	0.682	III	0.523	III
166	K638+193	K638+199	0.767	IV	0.188	I	0.144	II
167	K638+199	K638+226	0.767	IV	0.126	I	0.097	II
168	K638+226	K638+368	0.767	IV	0.532	III	0.408	III
169	K638+368	K638+409	0.767	IV	0.604	III	0.463	III
170	K638+409	K638+432	0.767	IV	0.205	I	0.157	II
171	K638+432	K638+444	0.767	IV	0.525	III	0.403	III
172	K638+444	K638+676	0.767	IV	0.173	I	0.133	II
173	K638+676	K638+837	0.767	IV	0.479	II	0.367	III
174	K639+837	K639+266	0.744	III	0.483	II	0.359	III
175	K639+266	K639+339	0.744	III	0.427	II	0.318	III
176	K639+339	K639+435	0.744	III	0.549	III	0.408	III
177	K639+435	K639+562	0.631	III	0.324	II	0.204	II
178	K640+562	K640+63	0.607	III	0.476	II	0.289	III
179	K641+63	K641+600	0.607	III	0.604	III	0.367	III
180	K642+600	K642+225	0.607	III	0.461	II	0.280	III